

CSGAN: Cyclic-Synthesized Generative Adversarial Networks for Image-to-Image Transformation

Kishan Babu Kancharagunta and Shiv Ram Dubey

Abstract—The primary motivation of Image-to-Image Transformation is to convert an image of one domain to another domain. Most of the research has been focused on the task of image transformation for a set of pre-defined domains. Very few works are reported that actually developed a common framework for image-to-image transformation for different domains. With the introduction of Generative Adversarial Networks (GANs) as a general framework for the image generation problem, there is a tremendous growth in the area of image-to-image transformation. Most of the research focuses over the suitable objective function for image-to-image transformation. In this paper, we propose a new Cyclic-Synthesized Generative Adversarial Networks (CSGAN) for image-to-image transformation. The proposed CSGAN uses a new objective function (loss) called Cyclic-Synthesized Loss (CS) between the synthesized image of one domain and cycled image of another domain. The performance of the proposed CSGAN is evaluated on two benchmark image-to-image transformation datasets, including CUHK Face dataset and CMP Facades dataset. The results are computed using the widely used evaluation metrics such as MSE, SSIM, PSNR, and LPIPS. The experimental results of the proposed CSGAN approach are compared with the latest state-of-the-art approaches such as GAN, Pix2Pix, DualGAN, CycleGAN and PS2GAN. The proposed CSGAN technique outperforms all the methods over CUHK dataset and exhibits the promising and comparable performance over Facades dataset in terms of both qualitative and quantitative measures. The code is available at <https://github.com/KishanKancharagunta/CSGAN>

I. INTRODUCTION

Recent advancements in image-to-image transformation problems, in which the image from one domain is transformed to the corresponding image of another domain. The domain specific problem has its applications in the fields of image processing, computer graphics and computer vision that includes image colorization [1], [2] image super-resolution [3], [4] image segmentation [5], [6] image style transfer [7], [8] and face photo-sketch synthesis [9], [10]. In this paper, a cyclic-synthesized generative adversarial network (CSGAN) is proposed for the image-to-image transformation. Fig. 1 highlights the improved performance of the CSGAN method for sketch to face synthesis compared to the latest state-of-the-art methods.

Traditionally, the above mentioned image-to-image transformation problems are handled by different transformation mechanisms [11], [15], as per the need. Even, some of the image-to-image transformation problems are dealt with other strategies such as classification, regression, etc. A multi-scale Markov random fields (MRF) based face photo-sketch

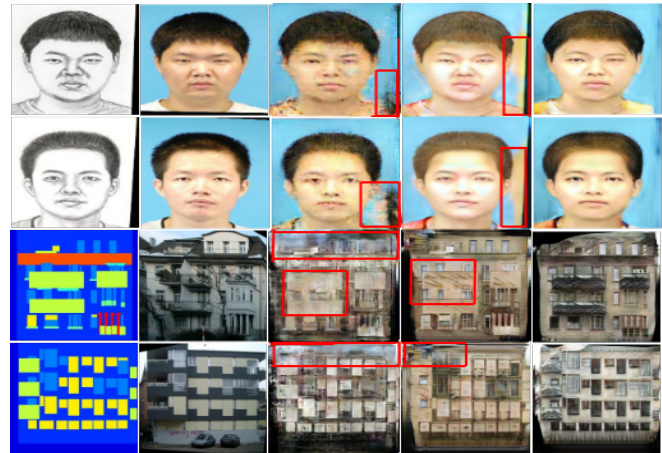


Fig. 1: Sample results from CUHK dataset [11] in 1st and 2nd rows and FACADES dataset [12] in 3rd and 4th rows. The 1st and 2nd columns show the input images and ground truth images, respectively. The 3rd, 4th, and 5th columns represent the transformed images using DualGAN [13], CycleGAN [14], and proposed CSGAN, respectively. Note that the artifacts in DualGAN and CycleGAN are marked with red color rectangles in 2nd and 3rd columns, respectively.

synthesis model is proposed to transfer the face sketch into a photo and vice-versa [11]. An image quilting method for texture synthesis is presented by [11] as an image transfer problem that uses patch based image stitching. A non local means method is proposed for image denoising based on an average of all pixel values in the image [15].

Later with the development of Deep Learning, Convolutional Neural Networks (CNNs) became very popular and widely used for different computer vision problems like object recognition [16], object localization [17], human action prediction [18] and medical image analysis [19]. The CNN based methods [20] and [7] for image-to-image transformation automatically learn the transformation function. It depends on the network architecture in the training phase with the given loss function. For example, [20] implemented a CNN based network for image colorization that uses Euclidean distance (i.e., L_2) as a loss function. A colorful image colorization network is designed by [2] which uses the multinomial cross entropy loss and gives better results compared to the [20] because of the averaging tendency of the Euclidean distance. [7] used combination of squared error and mean square error as the loss function for the image

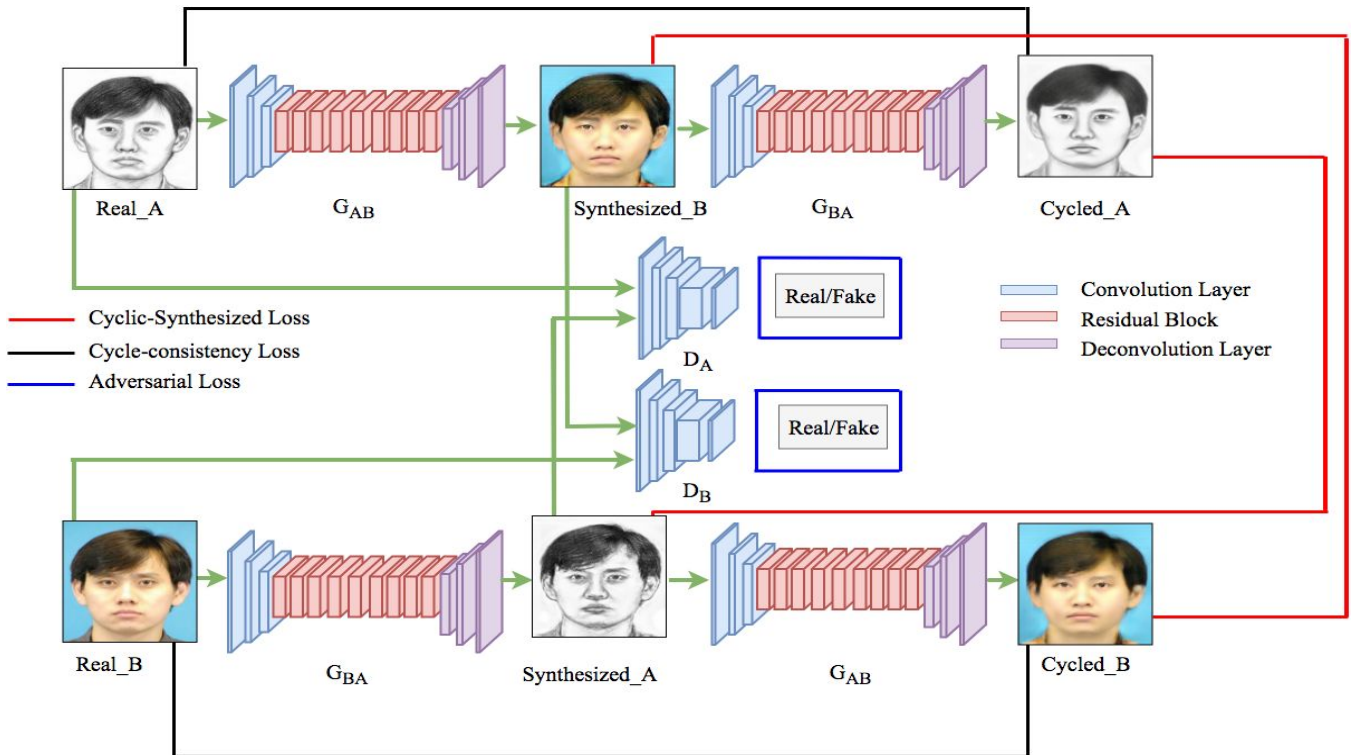


Fig. 2: Network architecture of the proposed CSGAN for image-to-image transformation. The cyclic-synthesized loss is proposed in this paper to utilize the relation between synthesized and cycled images in both the image domains. Thus, in addition to the adversarial loss and cycle-consistency loss, we have used cyclic-synthesized loss also to train the network. The adversarial loss is represented in the blue color rectangles which is calculated between 1) the generator G_{AB} and the discriminator D_B , and 2) the generator G_{BA} and the discriminator D_A . The cycle-consistency loss is shown in the black color and is calculated as L_1 loss between the real and cycled images. The cyclic-synthesized loss is shown in the red color and is calculated as L_1 loss between the synthesized and cycled images.

style transfer. Even though, the CNN based methods learn the transformation automatically, its performance depends on the selection of the loss functions that best suit for particular domain transformation.

Goodfellow et al. proposed the Generative Adversarial Network (GAN) for image generation in a given dataset [21]. It uses two networks, namely generator to generate the new samples and discriminator to distinguish between the generated and real samples. The competitive training of generator and discriminator is done such that the generator learns how to generate more realistic fake image, whereas the discriminator learns how to distinguish between the generated high quality fake image and real image. Generative Adversarial Networks (GANs) were initially proposed to generate models that are nearer to the training samples based on the given noise distribution. Later on the GANs were also used for different applications like image blending [22], semantic segmentation [23], single image super-resolution [24] and image inpainting [25], etc. These methods were introduced for particular applications, thus the generalized framework is still missing.

Isola et al. explored the Pix2Pix as the 1st common framework to work on image-to-image translation using Conditional GANs (cGANs) for paired image datasets [26]. Wang

et al. proposed a perceptual adversarial networks (PANs) for solving image-to-image transformation problems. The PANs combines the perceptual adversarial loss with the generative adversarial loss to solve this problem [27]. The perceptual adversarial loss of PAN enforces the network to learn the similarity between image pairs more semantically. Zhu et al. presented a framework with inverse mapping function for unsupervised data using Cycle-Consistent Adversarial Network (CycleGAN) [14]. The CyclicGAN transfer the images in two domains in both ways, i.e., in forward as well as in backward direction. Yi et al. developed a framework for image-to-image translation in an unsupervised setting using Dual-GAN mechanism [13]. Wang et al. proposed a framework for photo-sketch synthesis involving multi-adversarial networks (PS2MAN) [28].

In spite of the above mentioned recent developments, there are still gaps in terms of network architecture of the generator and discriminator, restrain on the size of the datasets and choice of the objective functions. The above mentioned network architectures mainly differ in terms of the loss functions used for the training. Most of the recent works included the Adversarial loss calculated between generators and discriminators, the Cycle-consistency loss calculated between the Real_Images and Cycled_Images, and

the Synthesized loss calculated between the Real_Images and Synthesized_Images. All these losses are used to minimize the gap between real and generated images. Even after considering all these losses, we still find the scope to minimize the loss between the Synthesized_Images and Cycled_Images. As per the best of our knowledge, no existing network utilizes the loss between the Synthesized_Images and Cycled_Images. Synthesized_Images are generated from the generators by giving Real_Images as the input and the same generators are used to generate the Cycled_Images by taking the Synthesized_Images as the input. In this paper, we propose a new loss function called as the Cyclic_Synthesized loss, which is first of its kind.

The contributions of this paper are mainly three-fold:

- We proposed a new loss function Cyclic-Synthesized Loss (CS Loss) that increases the quality of the results produced with reduced artifacts.
- We proposed the CSGAN architecture based on the CS Loss for image-to-image transformation.
- We evaluated our method over two benchmark datasets with baseline image quality assessment metrics and our method shows the better/comparable performance as compared to the state-of-the-art methods.

II. PROPOSED CSGAN ARCHITECTURE

In this section, first, we describe the problem formulation, followed by the depiction of the proposed method and its objective function. Later, the generators and discriminators architecture are discussed in detail.

For a given dataset $X \in \{(A_i), (B_i)\}_{i=1}^n$ which consists of the n number of the paired images of two different domains A and B , the goal of our method is to train two transformation functions, i.e., $G_{AB} : A \rightarrow B$ and $G_{BA} : B \rightarrow A$. The G_{AB} is a generator that takes a Real_Image (R_A) from domain A as the input and tries to transform it into a Synthesized_Image (Syn_B) of domain B . The G_{BA} is another generator that takes a Real_Image (R_B) in domain B as the input and tries to translate it into a Synthesized_Image (Syn_A) of domain A . In addition to the above two generators, the proposed method consists of two discriminators D_A and D_B to distinguish between R_A and Syn_A in domain A and R_B and Syn_B in domain B , respectively. The CycleGAN also used these two discriminators [14]. The real image of domain A , R_A and the real image of domain B , R_B are transformed into the synthesized image in domain B , Syn_B and synthesized image in domain A , Syn_A , respectively as,

$$Syn_B = G_{AB}(R_A) \quad (1)$$

$$Syn_A = G_{BA}(R_B) \quad (2)$$

The synthesized images (i.e., Syn_B and Syn_A) are again transformed into cycled images in another domain (i.e., Cyc_A and Cyc_B), respectively as,

$$Cyc_A = G_{BA}(Syn_B) = G_{BA}(G_{AB}(R_A)) \quad (3)$$

$$Cyc_B = G_{AB}(Syn_A) = G_{AB}(G_{BA}(R_B)) \quad (4)$$

The overall work of the proposed CSGAN method as shown in Fig. 2 is to transform image R_A from domain A to B by giving it to the generator network G_{AB} , results in the synthesized image Syn_B . The Synthesized image Syn_B from domain B and again transformed into the original domain A . by giving it to the generator network G_{BA} , results in the cycled image Cyc_A . In the same way the real image R_B from domain B is first transformed into the domain A as the synthesized image Syn_A and then transformed back into the domain B . as the cycled image Cyc_B by using the generator networks G_{BA} and G_{AB} , respectively. The discriminator network D_A is used to distinguish between the real image R_A and synthesized image Syn_A . In the same way, the discriminator network D_B is used to distinguish between the real image R_B and synthesized image Syn_B . To generate the synthesized images nearest to the real images, the loss between them is to be minimized. This signifies the need for efficient loss function.

A. Proposed Cyclic-Synthesized Loss

In this paper, the Cyclic-Synthesized loss is proposed to reduce the above mentioned artifacts. The generator network G_{BA} used to generate the Synthesized_Image Syn_A from the Real_Image R_B is also used to generate the Cycled_Image Cyc_A from the Synthesized_Image Syn_B . In a similar way, the generator network G_{AB} used to generate the Synthesized_Image Syn_B from the Real_Image R_A is also used to generate the Cycled_Image Cyc_B from the Synthesized_Image Syn_A as shown in Fig. 2. The distance between the Synthesized_Image and the Cycled_Image should be low as both are generated from the same generator. By this, the proposed Cyclic-Synthesized loss is calculated as L_1 loss between the Synthesized_Image (Syn_A) and the Cycled_Image (Cyc_A) in domain A and the Synthesized_Image (Syn_B) and the Cycled_Image (Cyc_B) in domain B . The Cyclic-Synthesized loss is defined as follows,

$$\mathcal{L}_{CS_A} = \|Syn_A - Cyc_A\|_1 = \|G_{BA}(R_B) - G_{BA}(G_{AB}(R_A))\|_1 \quad (5)$$

$$\mathcal{L}_{CS_B} = \|Syn_B - Cyc_B\|_1 = \|G_{AB}(R_A) - G_{AB}(G_{BA}(R_B))\|_1 \quad (6)$$

where the \mathcal{L}_{CS_A} is the Cyclic-Synthesized loss in domain A (i.e., between Syn_A and Cyc_A) and \mathcal{L}_{CS_B} is the Cyclic-Synthesized loss in domain B (i.e., between Syn_B and Cyc_B).

B. CSGAN Objective Function

The objective function (\mathcal{L}) for the proposed CSGAN method combines the proposed Cyclic-Synthesized loss with existing Adversarial loss and Cycle-consistency loss as follows,

$$\mathcal{L}(G_{AB}, G_{BA}, D_A, D_B) = \mathcal{L}_{LSGAN_A} + \mathcal{L}_{LSGAN_B} + \lambda_A \mathcal{L}_{cyc_A} + \lambda_B \mathcal{L}_{cyc_B} + \mu_A \mathcal{L}_{CS_A} + \mu_B \mathcal{L}_{CS_B} \quad (7)$$

where \mathcal{L}_{CS_A} and \mathcal{L}_{CS_B} are the proposed Cyclic-Synthesized loss explained in subsection II-A; \mathcal{L}_{LSGAN_A} , \mathcal{L}_{LSGAN_B} are the adversarial loss and \mathcal{L}_{cyc_A} , \mathcal{L}_{cyc_B} are the Cycle-consistency loss proposed in CycleGAN [14]. The adversarial loss and the Cycle-consistency loss are described in detail in following sub-sections:

1) *Adversarial Loss*: The generator networks $G_{AB} : A \rightarrow B$ and $G_{BA} : B \rightarrow A$ used in the proposed model are trained using the adversarial loss that comes from the discriminator against the generator network over a common objective function similar to the adversarial loss of original GAN [21]. The Generator network generates an image that looks similar to the original image, whereas the Discriminator distinguishes between the real and generated images. In this way both the Generator and discriminator networks are trained simultaneously by eliminating the problem of generating blurred images when L_1 or L_2 loss functions are used [26]. Similar to the CycleGAN [14], the least square loss introduced in [29], is used in the proposed method as the Adversarial loss. The least square loss stabilizes the training procedure to generate the high quality results. The adversarial loss between the Generator network G_{AB} and the Discriminator network D_B is computed as follows,

$$\mathcal{L}_{LSGAN_B}(G_{AB}, D_B, A, B) = \mathbb{E}_{B \sim P_{data}(B)}[(D_B(R_B) - 1)^2] + \mathbb{E}_{A \sim P_{data}(A)}[D_B(G_{AB}(R_A))^2]. \quad (8)$$

Similarly, the adversarial loss between the Generator network G_{BA} and the Discriminator network D_A is computed as follows,

$$\mathcal{L}_{LSGAN_A}(G_{BA}, D_A, B, A) = \mathbb{E}_{A \sim P_{data}(A)}[(D_A(R_A) - 1)^2] + \mathbb{E}_{B \sim P_{data}(B)}[D_A(G_{BA}(R_B))^2]. \quad (9)$$

where G_{AB} and G_{BA} are used to transform the images from $A \rightarrow B$ and $B \rightarrow A$, respectively, and D_A and D_B are used to distinguish between the original and transformed images in the domains of A and B , respectively. The Adversarial loss works as a good learned transformation function that can learn the distributions from the input images in training and generate similar looking images in testing. Even though Adversarial loss removes the problem of blurred images, still it produces the artifacts in the images due to the lack of the sufficient goodness measure.

2) *Cycle-consistency Loss*: The Cycle-consistency loss as discussed in [14] is also used in the objective function of the proposed method. It is calculated as L_1 loss between the Real Image (R_A) and the Cycled Image (Cyc_A) in domain A and the Real Image (R_B) and the Cycled Image (Cyc_B) in domain B . The Cycle-consistency loss is defined as follows,

$$\mathcal{L}_{cyc_A} = \|R_A - Cyc_A\|_1 = \|R_A - G_{BA}(G_{AB}(R_A))\|_1 \quad (10)$$

$$\mathcal{L}_{cyc_B} = \|R_B - Cyc_B\|_1 = \|R_B - G_{AB}(G_{BA}(R_B))\|_1 \quad (11)$$

where the \mathcal{L}_{cyc_A} is the Cycle-consistency loss in domain A (i.e., between R_A and Cyc_A) and \mathcal{L}_{cyc_B} is the Cycle-consistency loss in domain B (i.e., between R_B and Cyc_B).

We used L_1 distance instead of L_2 distance as the L_2 distance produces more blurred results when compared to the L_1 distance. The two losses \mathcal{L}_{cyc_A} and \mathcal{L}_{cyc_B} act as the forward and backward consistencies and introduce the constraints to reduce the space of possible mapping functions. Due to the large size of networks and with more mapping functions, the two losses serve the purpose of regularization while learning network parameters.

The above mentioned losses, i.e., Adversarial loss and Cycle-consistency loss used in CycleGAN [14] and DualGAN [13] produced good quality images. However, there is a need to minimize the artifacts produced as shown in Figure 1 for which we propose the Cyclic-Synthesized loss in this paper.

C. Network Architectures

In this paper, the Generator and Discriminator architectures are adapted from [14]. The Generator network, as shown in Table I consists of 3 Convolutional Layers followed by 9 residual blocks and 3 Deconvolutional Layers, is basically adapted from [8]. A brief description about the Generator and Discriminator networks are presented in this subsection. The used Discriminator network in the proposed method is a 70×70 PatchGAN taken from [26]. This network consists of the 4 Convolutional Layers, each one is a sequence of Convolution-InstanceNorm-LeakyReLU, followed by 1 Convolutional Layer to produce a 1 dimensional output as shown in Table II In the 1st convolutional layer, we do not use any normalization.

1) *Generator Architecture*: The Generator network, as shown in Table I consists of 3 Convolutional Layers followed by 9 residual blocks and 3 Deconvolutional Layers, is basically adapted from [8]. Instead of batch normalization we used instance normalization because in image generation networks the later one have shown great superiority over the previous one [14]. The input image of dimension 256×256 in source domain is given to the network. The network follows a series of down convolutions and up convolutions to retain the 256×256 in another domain.

2) *Discriminator Architecture*: The used Discriminator network in the proposed method is a 70×70 PatchGAN taken from [26]. This network consists of the 4 Convolutional Layers, each one is a sequence of Convolution-InstanceNorm-LeakyReLU, followed by 1 Convolutional Layer to produce a 1 dimensional output as shown in Table II In the 1st convolutional layer, we do not use any normalization.

The Discriminator network takes an image of dimension 256×256 and generates a probability of an image being either fake or real (i.e., a score between 0 for fake and 1 for real). The Leaky ReLUs with slope 0.2 is used as the activation function in the Discriminator network.

III. EXPERIMENTAL SETUP

This section, is devoted to present the experimental setup such as datasets, evaluation metric, training details and meth-

TABLE I: Generator Network Architecture. The r_p , s and p denote the size of reflection padding, stride, and padding, respectively.

Input:	Image (256x256)
[layer 1]	$r_p=3$; Conv2d (7, 7, 64), $s=1$; ReLU;
[layer 2]	Conv2d(3, 3, 128), $s=2$, $p=1$; InstanceNorm; ReLU;
[layer 3]	Conv2d (3, 3, 256), $s=2$, $p=1$; InstanceNorm; ReLU;
[layer 4]	$r_p=1$; Conv2d (3, 3, 256), $s=1$; InstanceNorm; ReLU; $r_p=1$; Conv2d (3, 3, 256), $s=1$; InstanceNorm;
[layer 5]	$r_p=1$; Conv2d (3, 3, 256), $s=1$; InstanceNorm; ReLU; $r_p=1$; Conv2d (3, 3, 256), $s=1$; InstanceNorm;
[layer 6]	$r_p=1$; Conv2d (3, 3, 256), $s=1$; InstanceNorm; ReLU; $r_p=1$; Conv2d (3, 3, 256), $s=1$; InstanceNorm;
[layer 7]	$r_p=1$; Conv2d (3, 3, 256), $s=1$; InstanceNorm; ReLU; $r_p=1$; Conv2d (3, 3, 256), $s=1$; InstanceNorm;
[layer 8]	$r_p=1$; Conv2d (3, 3, 256), $s=1$; InstanceNorm; ReLU; $r_p=1$; Conv2d (3, 3, 256), $s=1$; InstanceNorm;
[layer 9]	$r_p=1$; Conv2d (3, 3, 256), $s=1$; InstanceNorm; ReLU; $r_p=3$; Conv2d (3, 3, 256), $s=1$; InstanceNorm;
[layer 10]	$r_p=1$; Conv2d (3, 3, 256), $s=1$; InstanceNorm; ReLU; $r_p=1$; Conv2d (3, 3, 256), $s=1$; InstanceNorm;
[layer 11]	$r_p=1$; Conv2d (3, 3, 256), $s=1$; InstanceNorm; ReLU; $r_p=1$; Conv2d (3, 3, 256), $s=1$; InstanceNorm;
[layer 12]	$r_p=1$; Conv2d (3, 3, 256), $s=1$; InstanceNorm; ReLU; $r_p=1$; Conv2d (3, 3, 256), $s=1$; InstanceNorm;
[layer 13]	DeConv2d (3, 3, 128), $s=2$, $p=1$; InstanceNorm; ReLU;
[layer 14]	DeConv2d (3, 3, 64), $s=2$, $p=1$; InstanceNorm; ReLU;
[layer 15]	$r_p=3$; Conv2d (7, 7), $s=1$; Tanh;
Output:	Image (256x256)

TABLE II: Discriminator Network Architecture. The s and p denote the stride and the padding, respectively.

Input:	Image(256x256)
[layer 1]	Conv2d (4, 4, 64), $s=2$, $p=1$; LReLU;
[layer 2]	Conv2d (4, 4, 128), $s=2$, $p=1$; InstanceNorm; LReLU;
[layer 3]	Conv2d (4, 4, 256), $s=2$, $p=1$; InstanceNorm; LReLU;
[layer 4]	Conv2d (4, 4, 512), $s=1$, $p=1$; InstanceNorm; LReLU;
[layer 5]	Conv2d (4, 4, 1), $s=1$, $p=1$;
Output:	(Real/Fake) Score

ods compared.the datasets used in the proposed method are described first, followed by the description of the evaluation metrics, the training details of the proposed method and the GAN methods used for the results comparison.

A. DataSets

To appraise the efficiency of the proposed CSGAN method, we have evaluated the method on two publicly available datasets, namely CUHK and Facades. The subsection describes the datasets in brief.

1) *CUHK Student Dataset* : The CUHK¹ dataset consists of 188 face image pairs of sketch and corresponding face of students [11]. The cropped version of the CUHK dataset is used in this paper. The images are resized to the dimension of 256×256 from the original dimension of 250×200 . Among 188 images, 100 images are used for the training and rest for the testing.

¹<http://mmlab.ie.cuhk.edu.hk/archive/facesketch.html>

TABLE III: The average scores of the SSIM, MSE, PSNR and LPIPS metrics for the proposed CSGAN and latest state-of-the-art methods trained on CUHK Dataset.The values in bold highlights the best values, and the italic represents the next best.

Methods	Metrics			
	SSIM	MSE	PSNR	LPIPS
GAN	0.5398	94.8815	28.3628	0.157
Pix2Pix	0.6056	89.9954	28.5989	0.154
DualGAN	0.6359	<i>85.5418</i>	<i>28.8351</i>	0.132
CycleGAN	<i>0.6537</i>	89.6019	28.6351	0.099
PS2GAN	0.6409	86.7004	28.7779	<i>0.098</i>
CSGAN	0.6616	84.7971	28.8693	0.094

TABLE IV: The average scores of the SSIM, MSE, PSNR and LPIPS metrics for the proposed CSGAN and latest state-of-the-art methods trained on FACADES Dataset.The values in bold represents the best values, and the italic represents the next best.

Methods	Metrics			
	SSIM	MSE	PSNR	LPIPS
GAN	0.1378	103.8049	27.9706	0.252
Pix2Pix	<i>0.2106</i>	101.9864	28.0569	0.216
DualGAN	0.0324	105.0175	27.9187	0.259
CycleGAN	0.0678	104.3104	27.9489	0.248
PS2GAN	0.1764	<i>102.4183</i>	<i>28.032</i>	0.221
CSGAN	0.2183	103.7751	27.9715	<i>0.22</i>

2) *CMP Facades Dataset*: The CMP Facades² dataset has 606 image pairs of labels and corresponding facades with dimensions of 256×256 . The 400 image pairs are used for the training and remaining for the testing.

B. Evaluation Metrics

The quantitative as well as qualitative results are computed in this paper in order to get the better understanding of the performance of the proposed method. The Structural Similarity Index (SSIM) [30], Mean Square Error (MSE) and Peak Signal to Noise Ratio (PSNR) evaluation measures are adapted to report the results quantitatively. These evaluation measures are very common in image-to-image transformation problem to judge the similarity between the generated image and ground truth image. We also used the Learned Perceptual Image Patch Similarity (LPIPS) metric proposed by [31] and used in [32]. The LPIPS calculates the distance between the real and generated images by employing the more emphasis on perceptual similarity. The results are also depicted in the form of the produced images along with the real images for the qualitative comparison.

C. Training Information

From our observation, the default settings of CycleGAN [14] results in blurred images while trying to resize the input image from an arbitrary dimension to the fixed dimension 256×256 . The resultant blurred images ultimately causes the

²<http://cmp.felk.cvut.cz/~tylecr1/facade/>

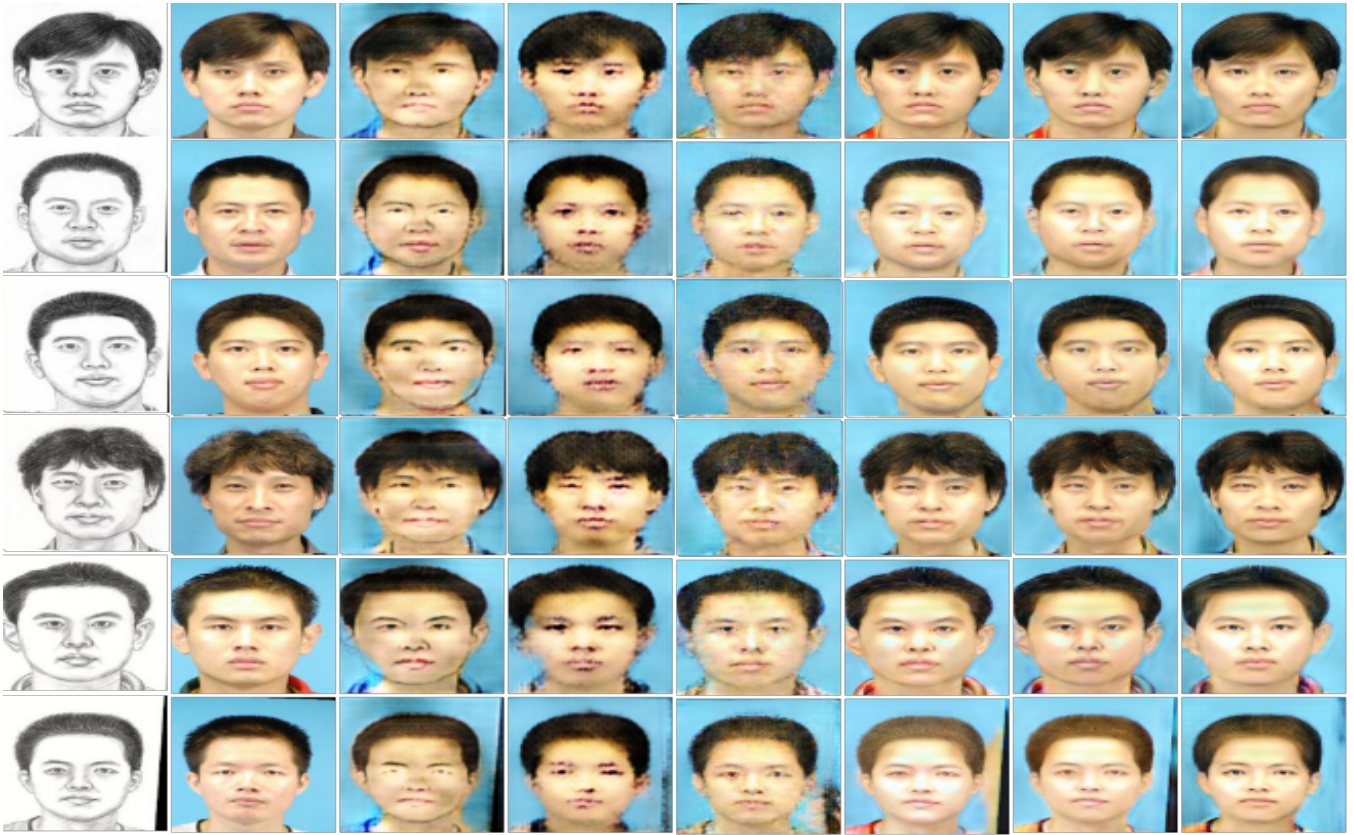


Fig. 3: Represents qualitative resemblance of sketch to photo transformation using CUHK dataset. From left to right: Input, Ground truth, GAN, Pix2Pix, DualGAN, CyclicGAN, PS2GAN and CSGAN. The CSGAN achieves lowest artifacts and generates the realistic and fair images.

deformations in the generated output images. So, in order to avoid this problem, the 256×256 dimensional images are used for the experiments in this paper. In each experiment, both the generator and discriminator networks are trained from scratch for 200 epochs with the batch size as 2. The Adam solver [33] is used in this experiment for training the networks with momentum term β_1 as 0.5. It is reported in [34] that the higher value of β_1 such as 0.9 can lead to poor stabilization. Initially, for the first 100 epochs, the learning rate is fix to 0.0002 and linearly decaying to 0 for next 100 epochs. To initialize the network weights, we have used the Gaussian Distribution with mean as 0 and standard deviation as 0.02. The joint training of generator and discriminator networks are performed. For the proposed CSGAN, the values of the weight factors λ_A and λ_B both are set to 10 and the values of the weight factors μ_A and μ_B both are set to 30 (see Equation 7). The default settings are used for the weight factors in compared methods as per the corresponding source paper. Two GPUs in parallel, namely PASCAL TITAN X (12GB)³ and GeForce GTX 1080 (8GB) are used for training the networks.

³Generously donated by NVIDIA Corp. through the Academic Partnership Program

D. Compared Methods

For analyzing the results the proposed CSGAN method is compared with five different state-of-the-art methods, namely GAN [21], Pix2Pix [26], DualGAN [13], CycleGAN [14] and PS2MAN [28]. For a fair comparison with the proposed CSGAN method as well as other methods, PS2MAN is implemented using a single adversarial network only i.e., PS2GAN. All these methods are compared with proposed method for paired image-to-image translation.

1) *GAN*: The original GAN was proposed for the new sample generation from the noise vector [21]. In this paper, the Pix2Pix⁴ [26] code is modified into GAN for image-to-image translation by removing the conditional property and L_1 loss.

2) *Pix2Pix*: The results are produced by using the code provided by the authors of Pix2Pix [26] with the same default settings.

3) *DualGAN*: The results are generated by using the code provided by the authors of DualGAN⁵ [13] with the same default settings.

4) *CycleGAN*: The results are obtained by using the code provided by the authors of CycleGAN⁶ [14] with the same

⁴<https://github.com/phillipi/pix2pix>

⁵<https://github.com/duxingren14/DualGAN>

⁶<https://github.com/junyanz/pytorch-CycleGAN-and-pix2pix>



Fig. 4: Qualitative comparison of labels to buildings transformation results on FACADES dataset. From left to right: Input, Ground truth, GAN, Pix2Pix, DualGAN, CycleGAN, PS2GAN, and CSGAN. The CSGAN generates the realistic and fair images with lowest artifacts.

default settings.

5) *PS2GAN*: The results are generated by modifying the original PS2MAN method proposed by [28], that uses a multiple adversarial networks. For a fair comparison with the proposed CSGAN method as well as other methods, PS2MAN is implemented using a single adversarial network only i.e., PS2GAN. The PS2GAN consists of the synthesized loss in addition to the losses mentioned in the CycleGAN [14].

IV. EXPERIMENTAL RESULTS AND ANALYSIS

In this section, results obtained by the proposed CSGAN method are compared against the five different base line image-to-image transformation methods like GAN, Pix2Pix, DualGAN, CycleGAN and PS2GAN. Both Quantitative and Qualitative analysis of the results are presented to reveal the improved performance of the proposed method.

1) *Quantitative Evaluation*: Table III and Table IV list the comparative results over the CUHK sketch-face and FACADES labels-buildings datasets, respectively using five different state-of-the-art methods along with the proposed CSGAN method. In terms of the average scores given by the SSIM, the MSE, the PSNR and the LPIPS metrics, the proposed CSGAN method clearly shows improved results over the other compared methods. It is also observed that

the proposed CSGAN generates more structurally and perceptually similar faces for a given sketch as it has highest value for SSIM and lowest value for LPIPS. The lowest value of MSE and highest value of PSNR points out that the proposed method generates the faces with more pixel level similarity. Thus, the proposed method is able to provide a very balanced trade-off between pixel-level similarity and structure/perceptual-level similarity.

In terms of structural similarity, i.e., the average SSIM score, the proposed CSGAN method outperforms the state-of-the-art GAN based methods. In terms of perceptual similarity, i.e., the proposed CSGAN is very close to the the best performing Pix2Pix method. One of the possible reason for it is due to the poor performance of adversarial loss itself. The performance improvement due to the proposed cyclic-synthesized loss (CS Loss) is dependent upon the performance of adversarial loss because the images used in CS Loss are not the original images, rather the synthesized and cycled images. It can be seen from the LPIPS results over FACADES dataset (see Table IV), that the LPIPS is poor for all the methods. For the FACADES dataset and in the context of the MSE and the PSNR metrics (i.e., the pixel-level similarity), the proposed method is not able to produce the best result due to the huge amount of difference between the labels and buildings domains.

2) *Qualitative Evaluation*: Fig. 3 and Fig. 4 show the qualitative comparison of the CSGAN results on CUHK and FACADES datasets, respectively, with five different state-of-the-art methods. The GAN, Pix2Pix and DualGAN are unable to generate the output even close to ground truth and contain the different type of artifacts such as face distortion, background patches, missing blocks, etc. The results of PS2GAN have the brightness inconsistency as well as missing patches in different samples. The results of CycleGAN is reasonably better, but still suffers with the color inconsistencies for different samples. These shortcomings are removed in the results of the proposed CSGAN method which are more realistic as compared to the other methods in terms of the shape, color, texture and reduced artifacts.

V. CONCLUSION

In this paper, we proposed a new method for image-to-image transformation called as CSGAN. The CSGAN is based on the Cyclic-Synthesized loss. Ideally, the cycled image should be similar to the synthesized image in a domain. The Cyclic-Synthesized loss finds the error between the synthesized and cycled images in both the domains. By adding the Cyclic-Synthesized loss to the objective function (i.e., other losses such as Adversarial loss and Cycle-consistency loss), the problem of unwanted artifacts is minimized. The performance of proposed CSGAN is validated over two benchmark image-to-image translation datasets and the outcomes are analyzed with the recent state-of-the-art methods. The thorough experimental analysis, confirms that the proposed CSGAN outperforms the state-of-the-art methods.

The performance of the proposed method is also either better or comparable over other datasets. In future we want to extend our work towards optimizing the generator and discriminator networks and to focus on unpaired datasets i.e., towards unsupervised learning

ACKNOWLEDGEMENT

The authors would like to thanks the NVIDIA Corp. for donating us the NVIDIA GeForce Titan X Pascal GPU used in this research.

REFERENCES

- [1] Z. Cheng, Q. Yang, and B. Sheng, "Deep colorization," in *IEEE International Conference on Computer Vision*, 2015.
- [2] R. Zhang, P. Isola, and A. A. Efros, "Colorful image colorization," in *European Conference on Computer Vision*, 2016.
- [3] T. Guo, H. S. Mousavi, and V. Monga, "Deep learning based image super-resolution with coupled backpropagation," in *IEEE Global Conference on Signal and Information Processing*, 2016, pp. 237–241.
- [4] J. Chen, X. He, H. Chen, Q. Teng, and L. Qing, "Single image super-resolution based on deep learning and gradient transformation," in *IEEE International Conference on Signal Processing*, 2016, pp. 663–667.
- [5] Z. Liu, X. Li, P. Luo, C.-C. Loy, and X. Tang, "Semantic image segmentation via deep parsing network," in *IEEE International Conference on Computer Vision*, 2015, pp. 1377–1385.
- [6] L.-C. Chen, Y. Yang, J. Wang, W. Xu, and A. L. Yuille, "Attention to scale: Scale-aware semantic image segmentation," in *IEEE conference on computer vision and pattern recognition*, 2016, pp. 3640–3649.

- [7] L. A. Gatys, A. S. Ecker, and M. Bethge, "Image style transfer using convolutional neural networks," in *Proceedings of the IEEE Conference on Computer Vision and Pattern Recognition*, 2016, pp. 2414–2423.
- [8] J. Johnson, A. Alahi, and L. Fei-Fei, "Perceptual losses for real-time style transfer and super-resolution," in *European Conference on Computer Vision*, 2016, pp. 694–711.
- [9] S. Zhang, X. Gao, N. Wang, J. Li, and M. Zhang, "Face sketch synthesis via sparse representation-based greedy search," *IEEE transactions on image processing*, vol. 24, no. 8, pp. 2466–2477, 2015.
- [10] L. Zhang, L. Lin, X. Wu, S. Ding, and L. Zhang, "End-to-end photo-sketch generation via fully convolutional representation learning," in *ACM International Conference on Multimedia Retrieval*, 2015, pp. 627–634.
- [11] X. Wang and X. Tang, "Face photo-sketch synthesis and recognition," *IEEE Transactions on Pattern Analysis & Machine Intelligence*, no. 11, pp. 1955–1967, 2008.
- [12] R. Tyleček and R. Šára, "Spatial pattern templates for recognition of objects with regular structure," in *German Conference on Pattern Recognition*, 2013.
- [13] Z. Yi, H. Zhang, P. Tan, and M. Gong, "Dualgan: Unsupervised dual learning for image-to-image translation," in *IEEE International Conference on Computer Vision*, 2017, pp. 2868–2876.
- [14] J.-Y. Zhu, T. Park, P. Isola, and A. A. Efros, "Unpaired image-to-image translation using cycle-consistent adversarial networks," in *IEEE International Conference on Computer Vision*, 2017, pp. 2242–2251.
- [15] A. Buades, B. Coll, and J.-M. Morel, "A non-local algorithm for image denoising," in *IEEE Conference on Computer Vision and Pattern Recognition*, 2005, pp. 60–65.
- [16] A. Krizhevsky, I. Sutskever, and G. E. Hinton, "Imagenet classification with deep convolutional neural networks," in *Advances in neural information processing systems*, 2012, pp. 1097–1105.
- [17] J. Tompson, R. Goroshin, A. Jain, Y. LeCun, and C. Bregler, "Efficient object localization using convolutional networks," in *IEEE Conference on Computer Vision and Pattern Recognition*, 2015.
- [18] S. Ji, W. Xu, M. Yang, and K. Yu, "3d convolutional neural networks for human action recognition," *IEEE transactions on pattern analysis and machine intelligence*, vol. 35, no. 1, pp. 221–231, 2013.
- [19] N. Tajbakhsh, J. Y. Shin, S. R. Gurudu, R. T. Hurst, C. B. Kendall, M. B. Gotway, and J. Liang, "Convolutional neural networks for medical image analysis: Full training or fine tuning?" *IEEE transactions on medical imaging*, vol. 35, no. 5, pp. 1299–1312, 2016.
- [20] Z. Cheng, Q. Yang, and B. Sheng, "Deep colorization," in *IEEE International Conference on Computer Vision*, 2015, pp. 415–423.
- [21] I. Goodfellow, J. Pouget-Abadie, M. Mirza, B. Xu, D. Warde-Farley, S. Ozair, A. Courville, and Y. Bengio, "Generative adversarial nets," in *Advances in neural information processing systems*, 2014, pp. 2672–2680.
- [22] H. Wu, S. Zheng, J. Zhang, and K. Huang, "Gp-gan: Towards realistic high-resolution image blending," *arXiv preprint arXiv:1703.07195*, 2017.
- [23] P. Luc, C. Couprie, S. Chintala, and J. Verbeek, "Semantic segmentation using adversarial networks," *arXiv preprint arXiv:1611.08408*, 2016.
- [24] C. Ledig, L. Theis, F. Huszár, J. Caballero, A. Cunningham, A. Acosta, A. P. Aitken, A. Tejani, J. Totz, Z. Wang *et al.*, "Photo-realistic single image super-resolution using a generative adversarial network," in *CVPR*, vol. 2, no. 3, 2017, p. 4.
- [25] D. Pathak, P. Krahenbuhl, J. Donahue, T. Darrell, and A. A. Efros, "Context encoders: Feature learning by inpainting," in *IEEE Conference on Computer Vision and Pattern Recognition*, 2016, pp. 2536–2544.
- [26] P. Isola, J.-Y. Zhu, T. Zhou, and A. A. Efros, "Image-to-image translation with conditional adversarial networks," in *IEEE Conference on Computer Vision and Pattern Recognition*, 2017, pp. 5967–5976.
- [27] C. Wang, C. Xu, C. Wang, and D. Tao, "Perceptual adversarial networks for image-to-image transformation," *IEEE Transactions on Image Processing*, vol. 27, no. 8, pp. 4066–4079, 2018.
- [28] L. Wang, V. Sindagi, and V. Patel, "High-quality facial photo-sketch synthesis using multi-adversarial networks," in *IEEE International Conference on Automatic Face & Gesture Recognition*, 2018, pp. 83–90.
- [29] X. Mao, Q. Li, H. Xie, R. Y. Lau, Z. Wang, and S. P. Smolley,

- “Least squares generative adversarial networks,” in *IEEE International Conference on Computer Vision*, 2017, pp. 2813–2821.
- [30] Z. Wang, A. C. Bovik, H. R. Sheikh, and E. P. Simoncelli, “Image quality assessment: from error visibility to structural similarity,” *IEEE transactions on image processing*, vol. 13, no. 4, pp. 600–612, 2004.
- [31] R. Zhang, A. A. Efros, E. Shechtman, and O. Wang, “The unreasonable effectiveness of deep features as a perceptual metric,” 2018.
- [32] J.-Y. Zhu, R. Zhang, D. Pathak, T. Darrell, A. A. Efros, O. Wang, and E. Shechtman, “Toward multimodal image-to-image translation,” in *Advances in Neural Information Processing Systems*, 2017, pp. 465–476.
- [33] D. P. Kingma and J. Ba, “Adam: A method for stochastic optimization,” *International Conference on Learning Representations*, 2014.
- [34] A. Radford, L. Metz, and S. Chintala, “Unsupervised representation learning with deep convolutional generative adversarial networks,” *arXiv preprint arXiv:1511.06434*, 2015.